

Rapid confocal Raman imaging using a synchro multifoci-scan scheme for dynamic monitoring of single living cells

Lingbo Kong,¹ Pengfei Zhang,¹ Jing Yu,¹ Peter Setlow,² and Yong-qing Li^{1,a)}

¹*Department of Physics, East Carolina University, Greenville, North Carolina 27858-4353, USA*

²*Department of Molecular, Microbial and Structural Biology, University of Connecticut Health Center, Farmington, Connecticut 06030-3305, USA*

(Received 10 March 2011; accepted 29 April 2011; published online 26 May 2011)

We developed a rapid multifoci-scan confocal Raman microscopy system for label-free molecular imaging of single living cells. A pair of galvo-mirrors were used to raster scan a single laser to generate multifoci excitations and another galvo-mirror synchronously projected Raman scattering from each foci onto a multichannel spectrograph such that multiple spectra were collected simultaneously. The image acquisition time is ~ 40 times faster than in conventional point-scan Raman microscopy with diffraction-limited resolution retained. We demonstrated that this system can be used to monitor the germination dynamics of single bacterial spores with about 1.0 min resolution and 2.5 mW power at each focal point. © 2011 American Institute of Physics.

[doi:10.1063/1.3595482]

Confocal Raman microscopy has proven to be a powerful molecular imaging technique for noninvasive studies of living cells.^{1,2} In conventional point-scan Raman microscopy, a laser point-focus under a microscope is raster scanned across the specimen in two dimensions (2D) and a full spectrum is confocally recorded at each x, y position. This point-to-point mapping affords the ultimate sensitivity, spatial resolution, image quality, and large spectral range capability.³ Due to the weak nature of Raman scattering of biomolecules, typical image acquisition times can be in order of 1–10 s per pixel (or longer) and thus total imaging times can be significant—it often takes tens of minute to obtain a Raman image of a living cell.^{4,5} This drawback limits the use of Raman scattering for *in vivo* imaging or monitoring fundamental processes of living cells, which requires imaging speeds of \leq tens of second per frame. In attempts to increase the imaging speed, efforts have been made to increase the Raman signals and thus decrease the acquisition times per pixel, including development of Raman imaging schemes using surface enhanced Raman scattering (SERS),^{2,6} coherent anti-Stokes Raman scattering (CARS),⁷ and stimulated Raman scattering (SRS).⁸ However, Raman imaging with SERS requires the injection of SERS nanoparticles into biological samples and CARS or SRS imaging generally uses one vibrational mode such that simultaneous imaging with a full spectrum is not an option. The other way to increase the speed of Raman imaging is the use of line-scan or multifoci-scan techniques.^{3,9,10} In line-scan Raman microscopy, a laser line focus (in the y direction) is raster scanned along the x axis and many spectra along the illumination line are recorded simultaneously using a charge coupled device (CCD) detector.^{3,9} However, the line-scan Raman mapping has low spatial resolution in the laser line direction. Recently, a multifocus confocal Raman microscopy technique has been developed to increase the imaging speed but retain the point-scan spatial resolution¹⁰ in which a sophisticated microlens array, pinhole array, and a fiber bundle are used to generate multifoci excitations and couple the Raman scattering in a

multichannel CCD detector. Since the separation of the adjacent foci is not adjustable and relatively large (2.0 μm), it is not suitable for the study of small microbial cells such as bacterial spores.⁵

In this letter, we report a multifoci-scan confocal Raman microscopy system that allows fast multimode vibrational images of living microbial cells. A pair of galvo-mirrors were used to raster scan a laser beam to generate multiple foci (~ 40) in one dimension or 2D arrays and a third galvo-mirror was used to synchronously project Raman scattering from different foci onto different pixel rows of a CCD chip so that full Raman spectra from each focus can be collected simultaneously in one measurement. Raman images were generated by scanning the foci array across the specimen. Beside the technical simplicity, the advantages of using synchro galvo-mirrors as the multifoci-scan scheme include: (1) the separation of multiple foci under the microscope is adjustable (down to ~ 100 nm) so that 1–2 μm living cells can be studied; (2) the separation of Raman scattering from adjacent foci on the CCD chip can be independently changed by the third galvo-mirror so that the cross-talk between adjacent foci can be reduced and point-scan confocal resolution can be retained; and (3) the image acquisition speed has been increased by a factor of ≥ 40 without taking the CCD readout time into account so that dynamic processes of living cells can be studied. This configuration of synchro galvo-mirrors has recently been used in multiple-trap laser tweezers Raman spectroscopy.¹¹

The schematic of the multifoci-scan confocal Raman imaging setup is shown in Fig. 1(a). A laser beam at 780 nm was introduced into an inverted microscope (Nikon TiS) equipped with an oil immersion objective (Plan Apo 60 \times , NA=1.40). A halogen lamp was used as the illumination source for bright-field or phase contrast imaging.^{12–14} A pair of galvo-mirrors GM₁ and GM₂ (Cambridge Technology, 6220H) were used to raster steer the incident laser beam step-by-step and generate 40 foci in 1 \times 40 or 2 \times 20 focus array under the microscope. Another galvo-mirror GM₃ (Thorlabs Inc., GVS001) in front of the spectrograph (Princeton Instruments, LS785) synchronously steered the

^{a)}Electronic mail: liy@ecu.edu.

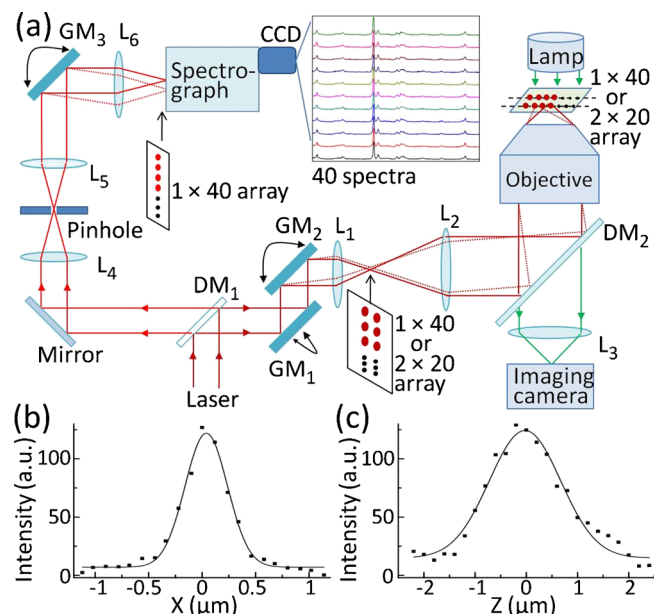


FIG. 1. (Color online) (a) Schematic of multifoci-scan confocal Raman imaging system. L: lens; GM: galvo-mirrors; and DM: dichroic mirrors. (b) Lateral and (c) axial intensity profiles of the Raman band at 1001 cm^{-1} of a 100 nm diameter polystyrene bead.

backward Raman scattering light from each focus point onto different vertical positions of a multichannel CCD chip (Princeton Instruments, PIXIS 400BR). The separations between foci on the sample and on the CCD were adjusted by changing the step-function voltages applied on GM₁ and GM₂, and the voltage applied on GM₃, respectively. The laser beam was raster-scanned across the 40 foci at a frequency of $\sim 10\text{ Hz}$ so that an effective foci-array excitation was created on the specimen and 40 spectra were collected within a CCD exposure time (1–10 s). The 400 CCD vertical pixels were divided into 40 parallel regions and only 3 pixels were binned as the sensing area in each region. The selection of 10-pixel separation was to avoid the potential crosstalk between Raman spectral spots from nearby foci. The vertical CCD binning and the width of the spectrograph's entrance slit formed an effective confocal pinhole ($60\text{ }\mu\text{m} \times 60\text{ }\mu\text{m}$) for Raman spectroscopy. We have measured the lateral and the axial resolution of our confocal Raman imaging system using a 100 nm diameter polystyrene bead. As shown in Figs. 1(b) and 1(c), the measured full-width at half-maximal intensity (FWHM) of the intensity profiles of Raman band at 1001 cm^{-1} in the lateral and axial direction were about $0.46\text{ }\mu\text{m}$ and $1.6\text{ }\mu\text{m}$, respectively. It shows that the Raman imaging system has high spatial resolution close to the diffraction limit. It should be noted that the axial resolution can be further improved by placing a pinhole and a pair of lens L₄ and L₅ in the optics path [Fig. 1(a)], as in point-scan confocal microscopy.

Raman spectra from each foci-array were collected with WINSPEC/32 software and spectral data analysis was processed in MATLAB. The smoothed backgrounds were first subtracted from the raw spectral data, and then a series of array spectra were corrected for the spectrograph's image aberration.¹⁵ The three-point Savitsky–Golay smoothing method was applied to reduce the noise of the spectral data before the intensities of specific Raman bands at each specimen position were extracted for multimode imaging. As a comparison between the performances of point-scan and

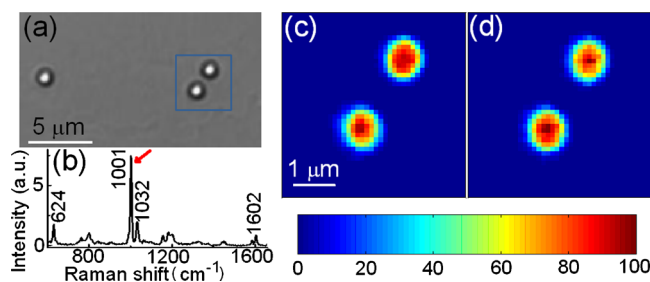


FIG. 2. (Color online) (a) Bright-field image of $1\text{ }\mu\text{m}$ diameter polystyrene beads adhered on a quartz coverslip. (b) Raman spectrum of the selected polystyrene bead. [(c) and (d)] Raman images (1001 cm^{-1} band) using point-scan (c) with 40 min acquisition time and multifoci-scan (d) with 1 min acquisition time of the two polystyrene beads; the laser power was 2.5 mW per pixel.

multifoci-scan schemes, we measured the Raman images (40×40 pixels at the 1001 cm^{-1} band) of two adjacent $1.0\text{ }\mu\text{m}$ polystyrene beads, as outlined in Fig. 2(a). Figure 2(c) shows the Raman image obtained from a point-scan scheme, in which the laser power was 2.5 mW at the single focus with 1.0 s of CCD exposure time (plus 0.5 s of readout time) per pixel and the total image acquisition time was about 40 min. Figure 2(d) shows the Raman image of the same polystyrene beads using multifoci-scan scheme with the image acquisition time of 1.0 min , in which the same laser power of 2.5 mW and the same CCD exposure time at each focus pixel were used (with the total incident power of 100 mW for per 40 spectra). By fitting the images in Figs. 2(c) and 2(d), we found that the FWHM of the polystyrene bead (bottom left) was $661 \pm 7\text{ nm}$ and the distance between two beads was $1.919 \pm 0.008\text{ }\mu\text{m}$ with the point-scan, in comparison to $662 \pm 7\text{ nm}$ and $1.921 \pm 0.008\text{ }\mu\text{m}$ with the multifoci-scan, respectively. This directly demonstrates that the multifoci-scan confocal scheme has similar high spatial resolution as the point-scan scheme.

Figure 3 shows that multifoci-scan confocal Raman microscopy can be used to generate multimode vibrational images of different Raman bands of various living cells, from which spatial information of different molecules in the same cells can be obtained simultaneously. Figures 3(c)–3(e) show images of human red blood cells (RBCs) (diameter of $6\text{--}8\text{ }\mu\text{m}$ and thickness of $2\text{ }\mu\text{m}$) with Raman bands at 752 ,

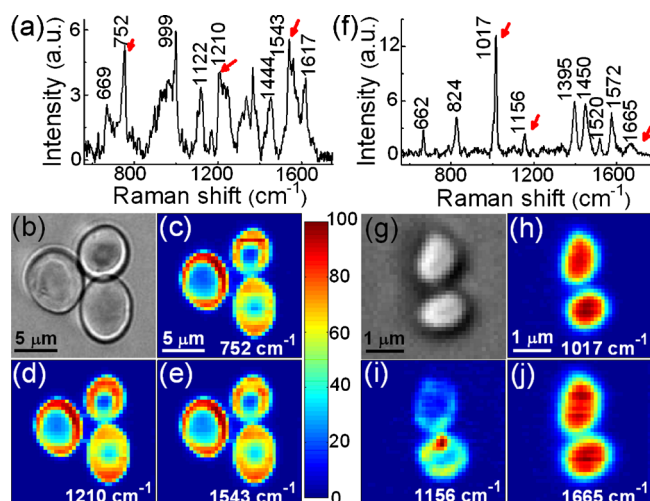


FIG. 3. (Color online) Raman spectra, bright-field images, and Raman images of human RBCs (a), (b), and (c)–(e), and dormant *Bacillus megaterium* spores (f), (g), and (h)–(j).

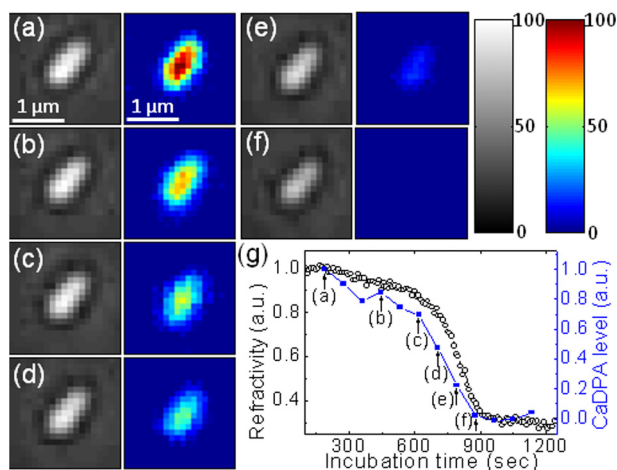


FIG. 4. (Color online) [(a)–(f)] Time-lapse phase contrast images (left) and Raman images (right) at the band of 1017 cm^{-1} of a single *Bacillus cereus* spore adhered on a quartz coverslip incubated with 5 mM L-alanine. (g) Refractivity (○) and CaDPA (■) as a function of the incubation time during germination; arrows indicate the times for acquiring the images of (a)–(f).

1210 , and 1543 cm^{-1} [Fig. 3(a)]. These bands correspond to the ν_{15} (porphyrin breathing), ν_{18} (C_mH), and ν_{11} ($C_\beta C_\beta$) vibration modes of hemoglobin, respectively.¹⁶ It is clear that the RBCs are donut-shaped, as shown in a bright field image [Fig. 3(b)]. The observed spatial distribution of hemoglobin inside the RBCs [see Figs. 3(c)–3(e)] confirms this characteristic shape.

The multimode Raman images of small living cells such as bacterial spores of *Bacillus megaterium* (with a size around $1\text{ }\mu\text{m}$) can also be obtained. Figure 3(f) shows the Raman spectrum of individual *B. megaterium* spores,^{12,13} including Ca-dipicolinic acid (CaDPA) bands at 662 , 824 , 1017 , 1395 , and 1572 cm^{-1} , carotenoid bands at 1156 and 1520 cm^{-1} , and protein amide band at 1665 cm^{-1} . CaDPA is considered to be located in the spore's central core where it comprises $\sim 25\%$ dry weight of the core while carotenoids are located in the spore's outer membrane.¹⁷ However, there are no Raman images that confirm this assignment. Figures 3(h)–3(j) show the multimode Raman images (40×40 pixels with a step of 100 nm) of *B. megaterium* spores, indicating that the carotenoids (1156 cm^{-1} band) are in the outer region of the spore while CaDPA (1017 cm^{-1} band) is in the central region. In addition, since the proteins are found throughout the spore, the protein image in Fig. 3(j) is slightly larger than the CaDPA image in Fig. 3(h). Note that the CCD exposure time was 8 s per foci-array of 40 spectra with a total power of 100 mW .

The capability of high speed and high resolution of multifoci-scan confocal Raman imaging technique makes it possible to monitor dynamic process of single living cells. We demonstrated this use of Raman imaging by studying of germination of single *Bacillus cereus* spores. For this purpose, we set the multifoci in a 2×20 array and it took 80 s to acquire a Raman image of 20×20 pixels ($2.3\text{ }\mu\text{m} \times 2.3\text{ }\mu\text{m}$), with an 8 s exposure time per array of 40 spectra. The left images of Figs. 4(a)–4(f) show the time-lapse phase contrast images of a *B. cereus* spore adhered on a quartz coverslip incubated in 5 mM L-alanine with 25 mM Tris-HCl buffer (pH 7.4) at $25\text{ }^\circ\text{C}$. The spores were heat shocked for 30 min at $65\text{ }^\circ\text{C}$ before the experiment.^{12,13} Dor-

mant spores appear phase bright due to the high refractive index in the spore core and nutrient molecules cause spore germination by triggering the release of small molecules including CaDPA and their replacement of with water so that germinated spores appear phase dark.^{12,17} Figure 4(g) (black circle) shows the change in the spore's refractivity (the sum of the phase-contrast image intensity) versus the incubation time. The right images of Figs. 4(a)–4(f) show the corresponding time-lapse Raman images of the 1017 cm^{-1} CaDPA band. This gives the spatial distribution of CaDPA during germination of an individual spore. Figure 4(g) (blue square) also shows the release of CaDPA during the incubation, which was the sum of Raman images of 1017 cm^{-1} band. The data in Fig. 4 were consistent with our findings that the completion of CaDPA release precisely corresponds to the end of the rapid drop in spore's refractivity^{12–14} but with rich spatial information.

In summary, we have developed a multifoci-scan confocal Raman microscopy system by using a simple synchro scanning galvo-mirror technique to realize fast Raman imaging while retaining point-scan resolution. The Raman images of different vibrational bands of relatively large human RBC and small *Bacillus* spores have been generated with this technique. The increase in the imaging speed enables us to monitor the germination of a single spore through Raman imaging with a time resolution of $\sim 1.0\text{ min}$. In addition, use of an electron multiplying CCD camera in the spectrograph could significantly increase the sensitivity^{10,18} and thus imaging speeds can be further increased.

This work was supported by a grant from the Army Research Office (YQL/PS) via contract No. W911NF-08-1-0431 and by a Multi-University Research Initiative (MURI) award from the Department of Defense (PS/YQL).

- ¹G. J. Puppels, in *Fluorescent and Luminescent Probes for Biological Activity*, edited by W. T. Mason (Academic Press, London, 1999).
- ²S. Keren, C. Zavaleta, Z. Cheng, A. de la Zerda, O. Gheysens, and S. S. Gambhir, *Proc. Natl. Acad. Sci. U.S.A.* **105**, 5844 (2008).
- ³S. Schlucker, M. D. Schaeberle, S. W. Huffman, and I. W. Levin, *Anal. Chem.* **75**, 4312 (2003).
- ⁴N. Uzunbajakava, A. Lenferink, Y. Kraan, E. Volokhina, G. Vrensen, J. Greve, and C. Otto, *Biophys. J.* **84**, 3968 (2003).
- ⁵P. Lasch, A. Hermelink, and D. Naumann, *Analyst (Cambridge, U.K.)* **134**, 1162 (2009).
- ⁶J. R. Lombardi and R. L. Birke, *J. Phys. Chem. C* **112**, 5605 (2008).
- ⁷C. L. Evans, E. O. Potma, M. Puoris'haag, D. Côté, C. P. Lin, and X. S. Xie, *Proc. Natl. Acad. Sci. U.S.A.* **102**, 16807 (2005).
- ⁸C. W. Freudiger, W. Min, B. G. Saar, S. Lu, G. R. Holtom, C. W. He, J. C. Tsai, J. X. Kang, and X. S. Xie, *Science* **322**, 1857 (2008).
- ⁹S. Bernard, O. Beyssac, and K. Benzerara, *Appl. Spectrosc.* **62**, 1180 (2008).
- ¹⁰M. Okuno and H. O. Hamaguchi, *Opt. Lett.* **35**, 4096 (2010).
- ¹¹P. F. Zhang, L. B. Kong, P. Setlow, and Y. Q. Li, *Opt. Lett.* **35**, 3321 (2010).
- ¹²L. B. Kong, P. F. Zhang, P. Setlow, and Y. Q. Li, *Anal. Chem.* **82**, 3840 (2010).
- ¹³L. B. Kong, P. F. Zhang, J. Yu, P. Setlow, and Y. Q. Li, *Anal. Chem.* **82**, 8717 (2010).
- ¹⁴L. B. Kong, P. F. Zhang, G. W. Wang, J. Yu, P. Setlow, and Y. Q. Li, *Nat. Protoc.* **6**, 625 (2011).
- ¹⁵Z. Huang, H. Zeng, I. Hamzavi, D. I. McLean, and H. Lui, *Opt. Lett.* **26**, 1782 (2001).
- ¹⁶B. R. Wood, B. Tait, and D. McNaughton, *Biochim. Biophys. Acta* **1539**, 58 (2001).
- ¹⁷P. Setlow, *Curr. Opin. Microbiol.* **6**, 550 (2003).
- ¹⁸T. Dieing and O. Hollricher, *Vib. Spectrosc.* **48**, 22 (2008).